ELSEVIER

Chemical Engineering Journal 134 (2007) 256–261

Chemical Engineering Journal

www.elsevier.com/locate/cej

Kinetics of phenol oxidation over hypercrosslinked polystyrene impregnated with Pt nanoparticles

V.Yu. Doluda [a,*], E.M. Sulman [a], V.G. Matveeva [a], M.G. Sulman [a], N.V. Lakina [a], A.I. Sidorov [a], P.M. Valetsky [b], L.M. Bronstein [c]

[a] *Tver State University, Tver, Russia*
[b] *A.N. Nesmeyanov Institute of Organoelement Compounds, Russian Academy of Science, Moscow, Russia*
[c] *Indiana University, Department of Chemistry, Bloomington, IN 47405, USA*

Abstract

Liqiud-phase catalytic wet-air oxidation (CWAO) of phenolic compounds is one of the most prospective methods of waste water purification at high concentrations of toxic phenolic compounds. In this work the synthesis and catalytic properties of mixed platinum-containing nanoparticles stabilized in polymeric matrix of hypercrosslinked polystyrene are discussed. The size of platinum nanoparticles was determined by transmission electron microscopy. Proposed catalytic system showed the high activity, selectivity and stability in the phenol CWAO. The optimal conditions of phenol oxidation leading to the selectivity of 98–99% at 99% conversion were determined and the kinetics of the process at various catalyst loadings, substrate concentrations, and temperatures was studied. Mathematical modelling of the process was carried out allowing the calculation of the reaction network model.

Keywords: Phenol oxidation; Hypercrosslinked polystyrene; Pt nanoparticles

1. Introduction

Continuous growth and development of industry lead to the constant increase of environmental pollution. Hydrological system undergoes the highest ecological burden. Highly toxic compounds get into water basins used for domestic purposes. Thus, the paramount objective of modern ecology is preserving water resources, i.e., prevention of pollution and/or purification of water from highly toxic organic compounds. Phenol and its homologues are in the group of the most hazardous organic pollutants [1,2], and they are difficult to decompose. Phenol can inhibit the biosynthesis of microorganisms, thus the self-cleaning of water cannot be done. At present to eliminate phenolic compounds, several methods are used such as extraction, sorption, membrane separation, and biological purification. However, none of the above methods allows effective elimination of phenol due to incomplete purification, large amounts of side-products, high energy consumption and consequently high cost of purification [3–6]. Liqiud-phase catalytic wet-air oxidation (CWAO) of phenolic compounds is one of the most prospective methods of waste water purification at high concentrations of toxic phenolic compounds [7].

Modern catalytic systems allow deep conversion of phenolic compounds to carbon dioxide and water [7–23], however the oxidation process is rather complicated due to large amount of intermediates (Fig. 1), some of which have low reactivity [8].

Depending on reaction conditions, several desirable and undesirable processes may occur: (i) full mineralization of phenolic compounds with formation of CO_2 and H_2O, (ii) formation of polymers, which can be easily separated from aqueous media by filtration, coagulation or flotation and (iii) formation of easily biodegradable compounds such as carboxylic acids, which however may lead to leaching of active metal from catalytic surface and its deactivation [9]. The most desirable path is the complete catalytic oxidation of phenols with formation of CO_2 and H_2O. For this reaction, the efficient and selective catalytic system should be developed and optimal reaction conditions should be chosen. The catalysts synthesized have to provide a high oxidation rate of phenolic pollutants and effective oxidation of broad-spectrum compounds with various functional groups. On top of that low cost and high mechanical and chemical stability (without significant loss of catalytic properties) have to be provided.

* Corresponding author at: A. Nikitina Str. 22, 170026 Tver, Russia. Tel.: +7 4822 449317; fax: +7 4822 449317.
E-mail address: sulman@online.tver.ru (V.Yu. Doluda).

1385-8947/$ – see front matter © 2007 Elsevier B.V. All rights reserved.
doi:10.1016/j.cej.2007.03.069

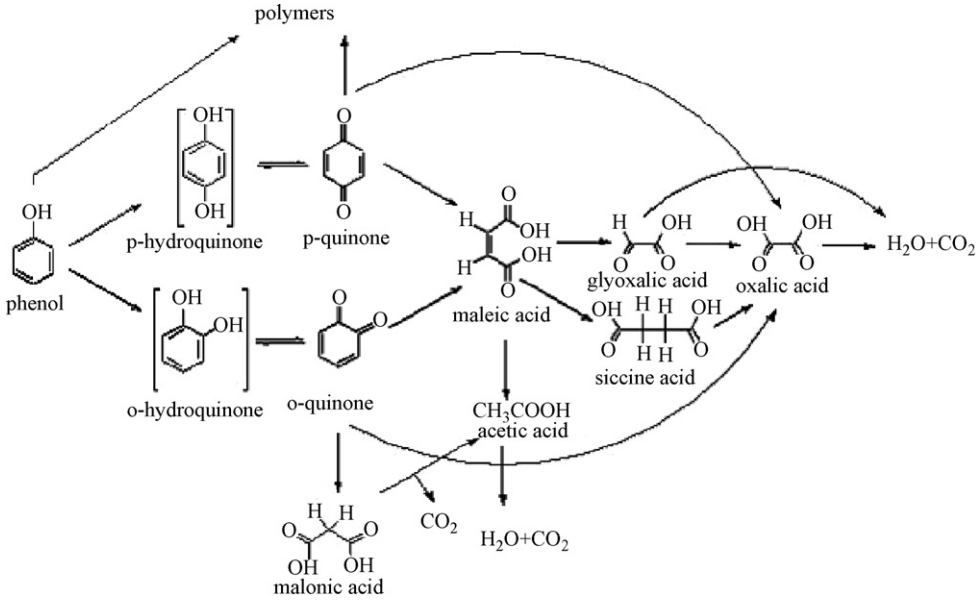

Fig. 1. The scheme of full phenol oxidation.

At present the catalytic oxidation of phenolic admixtures is carried out using air oxygen at 120–300 °C and 10–15 MPa over Fe, Cu, Ni, Co, Mn, Ti, and Pt catalysts [12,14,15,23–26]. The highest activity in oxidation of phenol and its homologues is shown by platinum catalysts deposited on various supports: activated carbon, γ-Al_2O_3, sibunit, TiO_2 [15,25]. Despite large variety of catalytic systems, none of them provide sufficient activity and selectivity leading to the required degree of conversion (95–99%). This inspires development of novel highly active, selective, and stable catalysts of liquid-phase phenol oxidation consisting of metal nanoparticles stabilized in nanostructured polymeric matrix [27]. The major advantage of these polymeric systems is the presence of nanostructures allowing control of nanoparticle growth and nanoparticle size distribution, along with modification of nanoparticle surfaces.

In this paper the structure of nanostructured catalyst based on hypercrosslinked polystyrene (HPS) and containing Pt nanoparticles and it catalytic properties in CWAO of phenol are reported.

2. Experimental

2.1. Catalyst synthesis and characterization

HPS was generously provided by Purolite Int. (UK), as Macronet MN 270/386-101/100 (hereafter designated as MM-HPS), and was used without further purification. To prepare Pt-containing MM-HPS, the polymer sample was impregnated with a predetermined amount of a $H_2PtCl_6{\cdot}6H_2O$ solution in THF [28]. The platinum content in the catalyst is 5 wt.% (MM-HPS-Pt).

The surface area of Pt-containing MM-HPS samples was obtained from nitrogen adsorption measurements using BECMAN COULTER^{TM} SA 3100^{TM} (Coulter Corporation, Miami, FL). Transmission electron microscopy (TEM) was performed with a JEOL JEM1010 electron microscope operated at accelerating voltage of 80 kV as described elsewhere [28]. X-ray photoelectron spectroscopy (XPS) analysis of MM-HPS-Pt was carried out with X-ray photoelectron analyzer "ES 2403 MT SCB AA RAS" (supplied by the Institute for Analytic Instrumentation of Russian Academy of Sciences, St. Petersburg, Russia) using Mg Kα ($h\nu$ = 1253.6 eV) in vacuum 10^{-9} Pa. X-ray fluorescence analysis (XRFA) was performed with Spectroskan Max (Infralum Inc., Russia). The Pt content in MM-HPS-Pt was determined using internal platinum standard.

2.2. CWAO of phenol

The catalytic reactions have been carried out in a glass batch isothermal reactor equipped with a stirrer (maximum 1200 rpm). The reactor was also equipped with two inlets: for catalyst, solvent, and substrate loading and for oxygen feeding. Before the substrate was charged into the reactor, the catalyst had been pretreated with O_2 for 60 min. Phenol initial concentration (C_0), catalyst amount (C_c) and oxidation temperature (t_h) were varied.

The analysis of the reaction mixture was carried out using HPLC chromatograph using stainless steel column 200 mm × 2 mm. The column was filled with a solid-phase C18, the liquid phase was a mixture of acetonitrile and water [13,32].

3. Results and discussion

3.1. Catalyst characterization

Hypercrosslinked polystyrene is the first representative of a new class of crosslinked polymers, which has unique topology and unusual properties [29,30]. The advantage of HPS is that it can serve both as nanostructured matrix controlling the

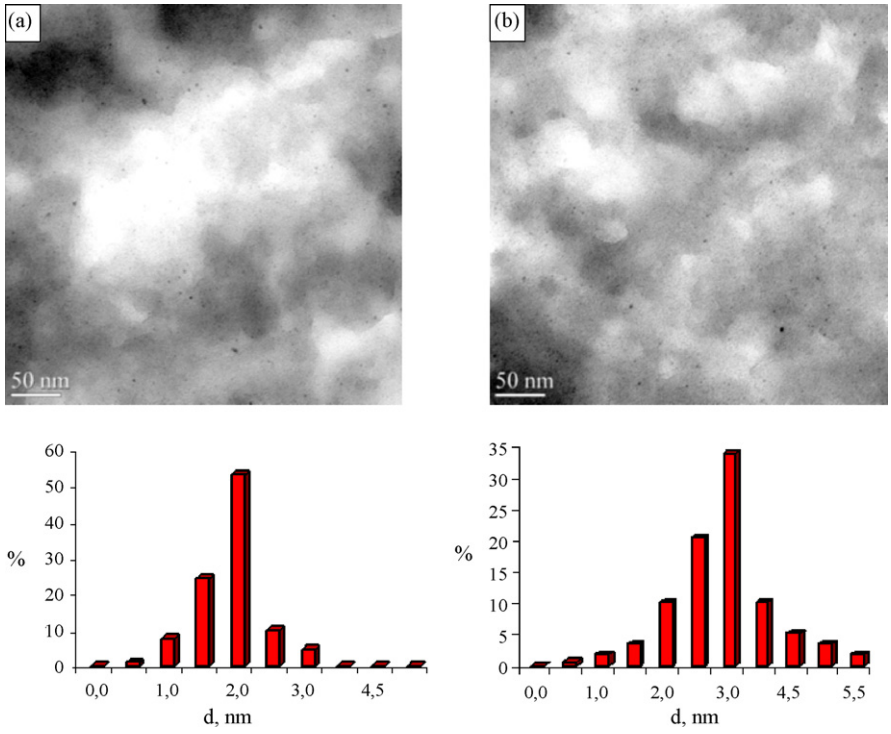

Fig. 2. TEM images and histograms of MM-HPS-Pt before (a) and after (b) CWAO.

nanoparticles growth, and the support of catalytic nanoparticles. Moreover, HPS is able to swell almost in all kinds of solvents, thus the access to catalytic sites is allowed in all reactive media including water. The HPS sample used here (MM-HPS) contains both micro- and mesopores (up to 22 nm). The latter facilitates the mass transfer of both reactants and products. As discussed elsewhere [28], incorporation of the THF solution containing platinic acid into HPS results in partial reduction of the Pt(IV) species and the formation of Pt(II) complexes wherein ligands are the products of the THF oxidation. These complexes form clusters (nanoparticles) in the MM-HPS pores. Fig. 2 presents the TEM micrographs and histograms of these images of MM-HPS-Pt before (Fig. 2a) and after the first catalytic oxidation (Fig. 2b). One can see that a mean nanoparticle diameter changes from 2.2 to 3.5 nm, revealing possible swelling of nanoparticles with the reaction components.

The XPS spectra of MM-HPS-Pt before and after first and fifth (five consecutive reactions were carried out to check the catalyst stability) catalytic reactions show (Fig. 3a) the existence of C, Cl, and Pt on the surface of the catalysts. (The Cl presence is due to unreacted CH_2Cl groups in the HPS synthesis.) After the first catalytic oxidation the decrease of the Pt content on the catalyst surface is observed (Table 1), while after the fifth reaction, the Pt content remains unchanged compared to that after the first reaction. Fig. 3b–d presents high resolution Pt XPS spectra (and their deconvolution) of the initial MM-HPS-Pt and the same catalyst after the first and fifth catalytic reactions. The fractions of each type of Pt species calculated from the deconvolution profiles are presented in Table 1. From these data one can see that the initial catalyst contains nearly equal amounts of Pt(IV) and Pt(II) species, while after the first catalytic reaction the Pt(II) species prevail. This should be due to reduction of Pt species with phenol during CWAO. No additional changes are observed after five repeating catalytic reactions.

3.2. Catalytic properties

The optimal conditions for phenol oxidation with MM-HPS-Pt have been identified by systematically varying the following reaction parameters: (i) catalyst concentration (C_c) from 5.15×10^{-4} to 5.15×10^{-2} M Pt, (ii) phenol concentration (C_0) from 0.0425 to 0.425 M, (iii) reaction temperature (T) from 40 to 95 °C, (iv) oxygen flow rate (V_O) from 10^{-3} to 10^{-1} L/s, and (v) stirring rate from 200 to 1200 rpm. (All the experiments were conducted at ambient oxygen pressure.) The highest selectivity obtained at 100% phenol conversion in this study is 98.5%. It is achieved with MM-HPS-Pt under the fol-

Table 1
Characteristics of Pt-containing MM-HPS-Pt by XPS

Catalyst notation	Pt species	(E ± 0.1) Pt $4f_{7/2}$ (eV)	Pt content (at.%)
MM-HPS-Pt	Pt(0)	71.5	1.9
	Pt(II)	73.6	48.3
	Pt(IV)	75.7	51.7
MM-HPS-Pt-first reaction	Pt(0)	71.6	12.9
	Pt(II)	72.9	67.5
	Pt(IV)	75.7	19.6
MM-HPS-Pt-fifth reaction	Pt(0)	71.4	15.6
	Pt(II)	72.9	69.4
	Pt(IV)	75.7	19.5

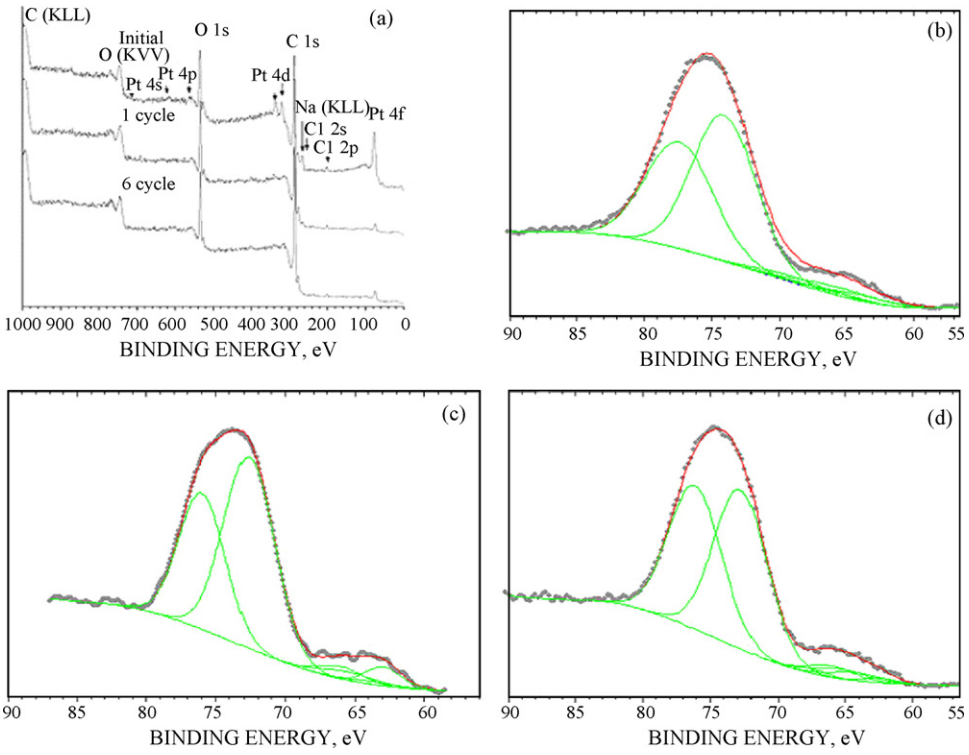

Fig. 3. (a) Survey XPS spectra of MM-HPS-Pt before and after the first and fifth catalytic reactions. High resolution Pt XPS spectra of MM-HPS-Pt before (b) and after the first (c) and fifth (d) catalytic reactions.

lowing reaction conditions: C_c 5.15×10^{-3} M Pt, C_0 0.21 M, T 95 °C, V_0 10^{-2} L/s, and stirring rate 1000 rpm.

The kinetic study of selective phenol oxidation with MM-HPS-Pt have been carried out at the substrate/catalyst concentration ratio ($q = C_0/C_c$) varied from 41.3 to 413 mol/mol Pt at a constant O_2 flow rate of 10^{-2} L/s and a stirring rate of 1000 rpm at 95 °C. The dependence of phenol conversion on reaction time is presented in Fig. 4. It demonstrates that an increase of C_0 at constant C_c promotes an increase in reaction time (t), which is typical for most catalysts.

The kinetic curves presented in Fig. 4 show that at the beginning of the reaction little or no phenol is consumed, suggesting the presence of an induction period when catalytic species are formed *in situ*. As a result of experimental data processing, the 50% phenol conversion time ($\tau_{0.5}$) has been determined. The value of $\tau_{0.5}$ was found to depend on the ratio $(C_0/C_c)^n$:

$$t_{0,5} \sim \left(\frac{C_0}{C_c}\right)^n \tag{1}$$

where n is the formal parameter characterizing the slope of the $\ln \tau_{0.5}$ dependence on $\ln (C_0/C_c)$.

For the catalytic system studied the parameter n is equal to two. This value is used for further mathematical modeling of the CWAO process.

HPLC analyses of the reaction products showed that the catalytic phenol oxidation with MM-HPS-Pt proceeds with high selectivity: the amount of intermediates in the reaction mixture does not exceed 1.5–2%, while the major reaction products are CO_2 and H_2O. A hierarchical approach of phenol degradation modeling would include several steps: (i) study of only phenol degradation (one-reaction network) to CO_2 and H_2O, (ii) modeling of carboxylic acid formation (five-reaction network), and finally (iii) incorporating all detected intermediates (eight-reaction network) [32]. Here the one-reaction network model was used because of a low fraction of intermediates. However, in the future a more detailed computation (ii and iii) will be performed to suggest a mechanistic hypothesis of phenol oxidation with MM-HPS-Pt [32].

The linear dependence of $\ln \tau_{0.5}$ on $\ln (C_0/C_c)$ allows us to introduce an independent variable, relative time:

$$\Theta = \frac{\tau}{(C_0/C_c)^n} \tag{2}$$

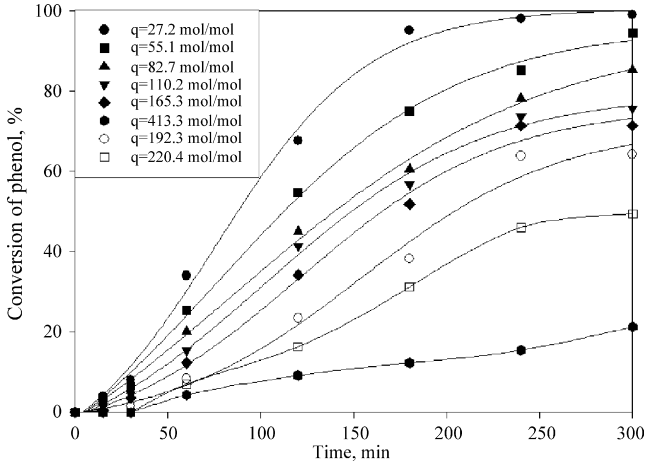

Fig. 4. The dependence of phenol conversion on time at various q.

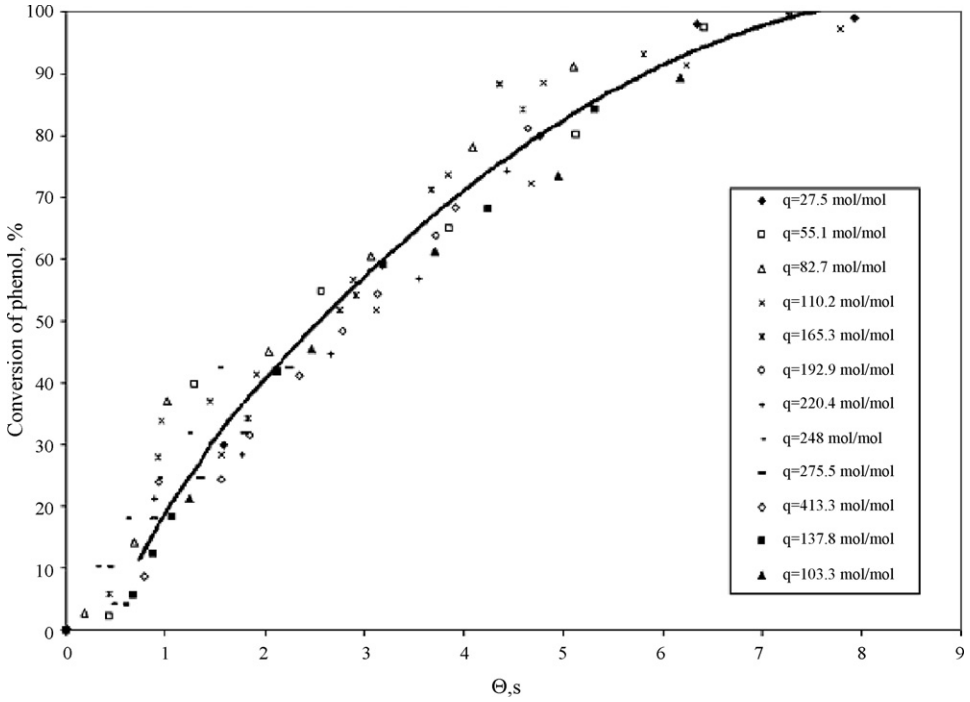

Fig. 5. Dependences of phenol conversion on relative time.

where τ is the current reaction time, n is equal to two (see above).

In so doing, the experimental data, presented in Fig. 4, have been brought together into a family of curves (Fig. 5) in the "phenol conversion, Θ" coordinates. This kinetic curve allows us to determine a mathematical model of phenol oxidation. For the computation, we have used the integral method using cubic spline and combined gradient method of Levenberg–Marquardt [31]. According to the results of the inverse problem solving, the kinetic model has been chosen that describes well the oxidation kinetics (the experimental plots correlate with the theoretical curve) (Fig. 5):

$$W = \frac{kx}{(x + Qx)^2} \tag{3}$$

Here x is the phenol concentration, k (1.1533 mol/(mol^2 s)) the kinetics parameter, and Q (1.826) is the adsorption parameter, taking into account the adsorption of the substrate with the catalyst; σ (3.12×10^{-2}) is the mean square deviation of computational curves from the experimental data.

This model describes the experimental data excluding the induction period (in the beginning of the reaction). The induction period can be described by a more complicated equation. The mathematical model (3) is a formal description of the one-reaction network of the phenol oxidation kinetics [32].

To calculate the parameters in the Arrhenius equation, the temperature of phenol oxidation was varied from 40 to 95 °C. Statistical analysis performed by the method described elsewhere [33] showed that within experimental error the adsorption parameter Q can be considered constant and independent on the temperature. From the experimental results the Arrhenius dependence was plotted in the coordinates $\ln k - 1/T$ and the apparent activation energy E_a was calculated [34]:

$$k = k_0 \, e^{-E/RT} \tag{4}$$

The activation energy of phenol oxidation with MM-HPS-Pt is 49 kJ/mol, which is lower than that (83 kJ/mol) of the conventional Pt catalyst on the alumina support with the same Pt content [23].

3.3. Investigation of the MM-HPS-Pt stability in CWAO of phenol

As is discussed above, the MM-HPS-Pt composition changes partially after the first catalytic reaction, but remains unchanged after the following four oxidations. This may suggest that the initial change is due to the formation of larger particles including phenol during the first oxidation, thus leading to the lower Pt content. The data presented in Table 2 show that the catalyst activity expressed as turnover frequency (TOF) and calculated as

$$\mathrm{TOF} = \frac{C(\mathrm{phen}) \times \alpha}{C(\mathrm{Pt}) \times t \times 100} \tag{5}$$

where α is the conversion degree (%) and t is the time (s) remains practically the same after 5 and even 10 consecutive catalytic reactions.

Table 2 shows the surface areas of MM-HPS and MM-HPS-Pt before and after the 1st, 5th, and 10th catalytic reactions. One can see that when the Pt species are incorporated into MM-HPS, the part of micropores is blocked by these species, leading to the considerable decrease of the BET surface area. On the other hand, after the first catalytic reaction the significant part of the micropore surface area is restored. It is likely that during

Table 2
Change of the platinum content and the catalyst surface area during repeated usage

No.	Catalyst	Pt content (wt.%)	BET surface area (m^2/g)	*t*-Plot surface area of micropores (m^2/g)	TOF ($\times 10^{-2}$ mol (phen)/(mol(Pt) s))
1	MM-HPS	–	1485	1099	–
2	MM-HPS-Pt	5.01	951	623	1.39
3	MM-HPS-Pt after 1 reaction	4.74	1232	991	1.24
4	MM-HPS-Pt after 5 reactions	4.71	1227	998	1.26
5	MM-HPS-Pt after 10 reactions	4.69	1240	1004	1.28

the first catalytic reaction, the formation of catalytically active nanoparticles occurs due to interaction with phenol and/or solvent and these nanoparticles are not blocking the micropore entrances. The following change in the platinum content and the surface area is almost negligible, revealing the high stability of the catalyst synthesized.

To make the MM-HPS-Pt-type catalysts relevant for a commercial use in CWAO of phenols, we will continue our studies, seeking conditions allowing a decrease of the Pt content and an increase of the O_2 pressure in CWAO of phenols. The preliminary experiments show that an increase of O_2 pressure during phenol oxidation leads to the increase of activity and the decrease of the process duration.

4. Conclusions

We have synthesized Pt-containing nanoparticles in pores of micro/mesoporous hypercrosslinked polystyrene and studied the behavior of this catalyst in liquid-phase CWAO of phenol. Formation of platinum clusters (nanoparticles) containing Pt(0), Pt(II), and Pt(IV) species occurs in the HPS pores due to interaction of platinic acid with THF. During the first catalytic reaction (phenol oxidation) the nanoparticle composition changes, leading to a higher fraction of the Pt(II) species, while the nanoparticle integrity is preserved. We believe that the compositional change is due to the interaction with phenol and inclusion of phenol or its oxidation products in the nanoparticle. The latter provide a π–π interaction of the nanoparticle ligands with the HPS pore walls and high stability of the catalysts during repeated usage. The size of the Pt-containing nanoparticles is 3.5 nm, leading to high catalytic activity. The catalytic system studied allows us to achieve nearly complete decomposition of phenol to non-hazardous compounds.

Acknowledgment

We sincerely thank NATO Science for Peace Programme SfP 981438 for financial support.

References

[1] C.Y. Chen, C.L. Lu, Sci. Tot. Environ. 289 (2002) 13.
[2] R. Guerra, Chemosphere 44 (2001) 1737.
[3] G. Jueptner, A method for wastewater treatment, US Patent 078,657 (2004).
[4] M.H. Entezari, C. Petrier, Appl. Catal. B: Environ. 53 (2004) 257.
[5] K. Yamada, Y. Akiba, M. Hirata, Chem. Sens. 20 (2004) 596.
[6] H. Gulyas, K. Breuer, B. Lindner, R. Otterpohl, Water Sci. Technol. 49 (2004) 241.
[7] Z.P.G. Masende, B.F.M. Kuster, K.J. Ptasinski, F.J.J.G. Janssen, J.H.Y. Katima, J.C. Schouten, Top. Catal. 33 (2005) 87.
[8] A. Cybulski, J. Trawczynski, Appl. Catal. B: Environ. 47 (2004) 1.
[9] N.M. Dobrynkin, M.V. Batygina, A.S. Noskov, P.G. Tsyrulnikov, D.A. Shlyapin, V.V. Schegolev, D.A. Astrova, B.M. Laskin, Top. Catal. 33 (2005) 69.
[10] J. Guo, M. Al-Dahhan, Chem. Eng. Sci. 60 (2005) 735.
[11] M. Abecassis-Wolfovich, M.V. Landau, A. Brinner, M. Herskowitz, Ind. Eng. Chem. Res. 43 (2004) 5089.
[12] A. Quintanilla, J.A. Casas, J.A. Zazo, A.F. Mohedano, J.J. Rodrigues, Appl. Catal. B: Environ. 62 (2006) 115.
[13] A. Santos, P. Yustos, B. Durban, F. Garcia-Ochoa, Catal. Today 66 (2001) 511.
[14] A. Santos, P. Yustos, B. Durban, F. Garcia-Ochoa, Top. Catal. 33 (2005) 181.
[15] P. Massa, F. Ivorra, P. Haure, R. Fenoglio, Catal. Lett. 101 (2005) 201.
[16] J. Wan, Y. Feng, W. Cai, S. Yang, X. Sun, J. Environ. Sci. 16 (2004) 556.
[17] I. Chen, S. Lin, C. Wang, L. Chang, J. Chang, Appl. Catal. B: Environ. 50 (2004) 49.
[18] L. Chang, I. Cheng, S. Lin, Chemosphere 58 (2005) 485.
[19] S. Kim, S. Ihm, Top. Catal. 33 (2005) 171.
[20] Z.P.G. Masende, B.F.M. Kuster, K.J. Ptasinski, F.J.J.G. Janssen, J.H.Y. Katima, J.C. Schouten, Catal. Today 79 (2003) 357.
[21] J.J. Barbier, L. Olivero, B. Renard, D. Dupez, Top. Catal. 33 (2005) 77.
[22] S. Yang, Y. Feng, W. Cai, W. Zhu, Z. Jiang, J. Wan, Rare Met. 23 (2004) 357.
[23] V.I. Demidyuk, S.N. Tkachenko, E.A. Makhov, V.V. Lunin, G.V. Egorova, I.S. Tkachenko, J.O. Che, R.N. Pyagai, S.I. Mun, Catal. Ind. 6 (2003) 42.
[24] Q. Wu, X. Hu, P.-L. Yue, Chem. Eng. Sci. 58 (2003) 923.
[25] C.I. Herrerias, T.Y. Zhang, C.J. Li, Tetrahedron Lett. 47 (2006) 13.
[26] D. Srinivas, S. Sivasanker, Catal. Surv. Asia 7 (2003) 121.
[27] L.M. Bronstein, in: H.S. Nalwa (Ed.), Encyclopedia of Nanoscience and Nanotechnology, vol. 7, APS, Stevenson Ranch, CA, 2004, p. 193.
[28] S.N. Sidorov, I.V. Volkov, V.A. Davankov, M.P. Tsyurupa, P.M. Valetsky, L.M. Bronstein, R. Karlinsey, J.W. Zwanziger, V.G. Matveeva, E.M. Sulman, N.V. Lakina, E.A. Wilder, R.J. Spontak, J. Am. Chem. Soc. 123 (2001) 10502.
[29] V.A. Davankov, M.P. Tsyurupa, React. Polym. 13 (1990) 27.
[30] M.P. Tsyurupa, V.A. Davankov, J. Polym. Sci.: Polym. Chem. Ed. 18 (1980) 1399.
[31] Y. Bard, SIAM J. Numer. Anal. 7 (1970) 157.
[32] A. Eftaxias, Catalytic wet air oxidation of phenol in trickle bed reactor: kinetics and rector modeling, Universitat Rovira i Virgili, Tarragona, 2002.
[33] S. Vajda, P. Valko, T. Turani, Int. J. Chem. Kinet. 17 (1985) 55.
[34] B.N. Sakakini, A.S. Verbrugge, J. Chem. Soc., Faraday Trans. 93 (1997) 1637.